Local tunneling spectroscopy of the electron-doped cuprate superconductor $Sm_{1.85}Ce_{0.15}CuO_4$

A. Zimmers,[1,2,*] Y. Noat,[1] T. Cren,[1] W. Sacks,[1] D. Roditchev,[1] B. Liang,[2] and R. L. Greene[2]
[1]*Institut des Nanosciences de Paris, CNRS UMR 7588, Campus Boucicaut, 140 rue de Lourmel, F-75015 Paris, France*
[2]*Center for Superconductivity Research, Department of Physics, University of Maryland, College Park, Maryland 20742, USA*
(Received 3 August 2007; published 8 October 2007)

We present local tunneling spectroscopy in the optimally electron-doped cuprate $Sm_{2-x}Ce_xCuO_4$, $x=0.15$. A clear signature of the superconducting gap is observed with an amplitude ranging from place to place and from sample to sample ($\Delta \sim 3.5-6$ meV). Another spectroscopic feature is simultaneously observed at high energy with an amplitude ranging from ±60 to ±80 meV. Its energy scale and temperature evolution are found to be compatible with previous photoemission and optical experiments. If interpreted as the signature of antiferromagnetic order in the samples, these results could suggest the coexistence on the local scale of antiferromagnetism and superconductivity on the electron-doped side of cuprate superconductors.

DOI: 10.1103/PhysRevB.76.132505 PACS number(s): 74.25.Gz, 74.72.Jt, 75.30.Fv, 75.40.−s

Due to strong correlations, doping a Mott insulator yields a number of fascinating properties in a great number of materials. Among these, understanding the properties of cuprates remains one of the greatest challenges in condensed matter physics. In recent years, an important effort has been made to understand the interplay between the antiferromagnetic (AF) and the superconducting orders. A close relation between these two is undeniably present on the electron-doped side of the phase diagram since both orders overlap in a narrow doping range. This observation was first reported by angle resolved photoemission spectroscopy (ARPES) when revealing the presence of a large energy gap on parts of the Fermi surface[1] in superconducting samples. The particular symmetry of this large energy gap, which happens at the interception between the nominal Fermi surface and the antiferromagnetic Brillouin zone, has led to its interpretation as the signature of AF order in the sample. The characteristic temperature T' below which this large energy gap opens has since been mapped out over the phase diagram by infrared spectroscopy,[2,3] revealing its presence up to $x=0.17$ in superconducting $Pr_{2-x}Ce_xCuO_4$ (PCCO) samples. However, neither ARPES nor infrared spectroscopy is able, in principle, to differentiate if this large energy gap is due to long range AF order or AF fluctuations. These techniques can only estimate at best the minimum fluctuation length and time scales involved. A recent inelastic neutron diffraction measurement[4] has resolved this issue by showing that in superconducting samples, the antiferromagnetic correlation length does not diverge but saturates at low temperatures. This suggests that only AF fluctuations are present with a characteristic length scale of 200 Å in optimally doped samples. An important challenge now is to see whether both orders do coexist on a local scale.

To answer this question, we report a set of local tunneling spectroscopy measurements in scanning tunneling microscopy (STM) geometry on the electron-doped cuprate $Sm_{1.85}Ce_{0.15}CuO_4$ (SCCO) on larger energy scales. The tunneling conductance spectra simultaneously show the superconducting gap at low energies and a high energy feature at the same spatial positions. The attribution of this high energy feature to the presence of local AF order suggests that in electron-doped cuprates, antiferromagnetism and superconductivity coexist locally at optimal doping. In addition to these various energy scales, our measurements have revealed no changes in the superconducting gap magnitude within a 330 Å map but show large variations of this gap (up to 70%) between distant points within the same sample and between two different optimally doped samples. These large variations could be explained by modulation of the cerium and oxygen content within the samples. This observation is different from previous scanning tunneling microscopy measurements in the hole-doped cuprate Bi-2212 which show local inhomogeneities in the superconducting gap on the nanoscale.[5,6]

Local electronic properties are probed by STM and/or scanning tunneling spectroscopy (STS), where the tunneling current $I(V)$ is measured between an atomically sharp tip and a sample as a function of the bias voltage. The tunneling junctions were achieved by approaching mechanically cut Pt/Ir tips [whose density of states (DOS) near the Fermi level is roughly constant] to the c-axis oriented surface of the crystals. This configuration is believed to be most sensitive to the DOS of the CuO_2 planes of SCCO. The differential conductance measured, dI/dV, is proportional to the sample local DOS convoluted with the Fermi function (at the energy E_F+eV).

Single crystals of $Sm_{2-x}Ce_xCuO_4$ were grown by the flux method. Samples were typically a few millimeters along the a and b axes and a few hundred microns along the c axis. Cerium concentrations were determined by wavelength dispersive x-ray analysis (WDX) and superconducting transition temperatures were measured by dc susceptibility. The two samples presented here are SCCO with cerium concentrations $x=0.145\pm0.005$ and an onset $T_c=20$ K and SCCO with $x=0.155\pm0.005$ and an onset $T_c=17.5$ K. These concentrations are simply indications of the carrier density in the samples since the carrier density can also slightly change due to various oxygen reduction treatments. The oxygen stoichiometry in this material is achieved by annealing the crystal under reduced oxygen environment for 3–5 days at 925 °C. It is not possible to exclude a slight variation of oxygen content within the crystal volume. Since the electronic properties of this material are very sensitive to oxygen content,[7] this could explain the variations of the superconducting gap we present even though both samples are near optimally doped in cerium. Finally, these materials were chosen since

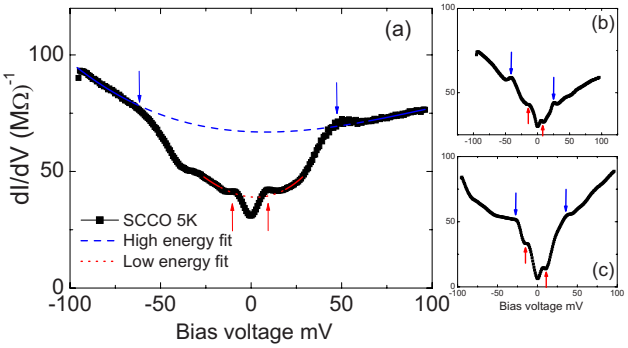

FIG. 1. (Color online) (a) Raw spectra at 5 K of SCCO with $x=0.145$ (onset $T_c=20$ K). Low and high energy features are identified by the red and blue (lower and upper) arrows. The red and blue fits were used in Figs. 2(a) and 2(b) to divide out the background. For the high energy background, the fitting region was chosen to be $[-180;-120]$ meV and symmetrically from $[120,180]$ meV. For the low energy background, the fitting region was chosen from $[-55;-35]$ meV and from $[35;55]$ meV. The intermediate region in both fits (see dashed blue and dotted red fits) was not used when evaluating the background fit but was used when normalizing the spectra of this figure to obtain Figs. 2(a) and 2(b). [(b) and (c)] Raw spectra on the same sample but at distant positions. The superconducting gap is always centered around zero bias as expected; however, we observe that the high energy feature can be shifted to negative [panel (b)] or to positive bias [panel (c)] depending on the location.

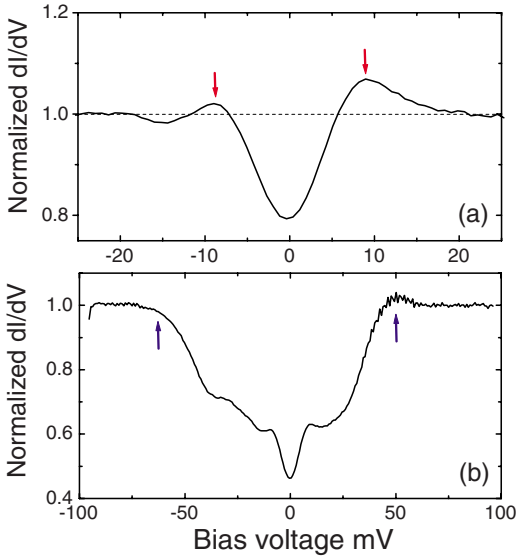

FIG. 2. (Color online) (a) Low energy feature isolated by dividing out the low energy background (see the dotted red fit in Fig. 1). This feature is identified as the superconducting gap and is found to have a magnitude of $2\Delta=12$ meV in a BCS picture. (b) High energy feature isolated by dividing out the high energy background (see the dashed blue fit in Fig. 1). The high energy feature magnitude is identifiable by the lower blue arrows.

they present the advantage of being cleavable compared to other electron-doped cuprates such as $Nd_{2-x}Ce_xCuO_4$ (NCCO) and PCCO. Our samples were thus cleaved *in situ* in ultrahigh vacuum and cooled down to 4.2 K immediately after.

In Fig. 1, we present a typical spectrum obtained at 5 K. One can distinguish a low energy feature (see lower red arrows). The shape and the temperature dependence of this feature allow us to identify it with the superconducting gap. The shape of the feature can be isolated in Fig. 2(a) when dividing out the "U" shaped background (see the dotted red fit in Fig. 1 named "low energy fit"). As discussed further, this background choice is the best representation of the spectra above T_c. By isolating the low energy feature in Fig. 2(a), one can then notice weak coherence peaks in the spectrum. These peaks are incompatible with the low energy pseudogap measured by tunnel junction measurements[8,9] but compatible with the signature of the superconducting gap. The zero-bias conductance (ZBC) value of 80% is slightly higher than other well studied cuprates such as $YBa_2Cu_3O_{7-\delta}$ (YBCO) where the ZBC is generally found to be around 50%. Using this spectrum, one finds the gap value from peak to peak to be $2\Delta_{pp}=18$ meV. In a BCS picture, this corresponds to a gap of $2\Delta=12$ meV. Using this extraction method, tunneling spectra measurements performed at various distant points on the same sample and on two different optimally doped samples show a superconducting gap 2Δ ranging from 7 to 12 meV. These variations could be explained by inhomogeneities on large scales in the oxygen content arising in the reduction process and/or variation of cerium concentration on the micron scale. Using these gap values, we find a ratio $2\Delta/k_BT_c$ varying from 4 to 7. Other spectroscopic techniques find this ratio to be 4.4 from Raman[10] in NCCO, 2.3 from photoemission in PLCCO,[11] 5 from optical conductivity of optimally doped PCCO,[12] 3.4 in NCCO and $Pr_{1-x}LaCe_xCuO_4$ (PLCCO) $x=0.11$ from point contact tunneling spectroscopy,[13] and 2.1–4 as a function of doping in a tunneling study of PCCO.[14] All of these ratios are on the lower limit of the one we find in SCCO. Figure 3 presents the temperature dependence from 5 to 300 K on a second optimally doped sample. When raising the temperature through the superconducting transition from 5 to 27 K, one observes that the low energy feature vanishes. All of the arguments described above allow us to identify this low energy feature with the superconducting gap.

We now discuss the high energy part of the spectra. Similar to the analysis used to isolate the superconducting gap, we have adjusted the conductance background above and below the high energy feature. This background fit presented in dashed blue in Fig. 1 is divided out to give Fig. 2(b). We have chosen the simplest background line (see the dashed blue fit in Fig. 1 named "high energy fit") in order to isolate the characteristic energy scale of the high energy feature. Note that such a U shaped background is also observed in many other superconducting cuprates such as YBCO. The magnitude of the high energy feature is identified to be $2\Delta'=120$ meV [see upper blue arrows in Fig. 1 and lower blue arrows in Fig. 2(b)]. This value is comparable in magnitude with the large energy pseudogap measured by ARPES[1,15] and optical spectroscopy in NCCO,[2] PCCO,[3] and SCCO.[15] However, further quantitative comparison is hard to pursue since the estimate of the large energy pseudogap magnitude clearly depends on the spectroscopy technique used. Indeed, a recent study on a unique underdoped SCCO

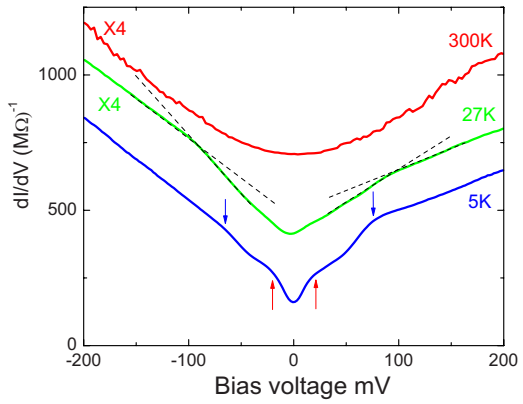

FIG. 3. (Color online) Temperature evolution of the tunneling spectra of SCCO with $x=0.155$ (onset $T_c=17.5$ K) at 5, 27, and 300 K (the 27 and 300 K curves are multiplied by 4 for clarity). The superconducting gap seen at 5 K (see lower red arrows) is found to be closed at 27 K which is above T_c. The high energy feature is, however, still present (see upper blue arrows and dashed lines as a guide for the eye). The high energy feature is found to be closed at room temperature. Using previous optical results, the high energy characteristic temperature T' is estimated to be 130 K, well above 27 K and well below 300 K.

sample[15] has shown that the estimate of the large energy pseudogap varies from 200 to 300 meV when measuring, respectively, by photoemission or optical conductivity. The most interesting and controversial aspect of our STM spectra is the observation of the superconducting gap and large energy pseudogap at the same local measurement points. The resolution of the tip was evaluated to be 10 Å. The vast majority of data recorded using various samples showed both gaps in each spectrum. If the high energy feature is identified to be the signature of an antiferromagnetic order in the sample, this would then imply that both superconductivity and antiferromagnetism could coexist locally.

The spectra shown in Fig. 1(a) present the advantage of being symmetric with respect to the zero-bias voltage. This symmetry is not always present in the data. Indeed, in many spectra, the high energy features were shifted to one or the other side of the zero-bias voltage [see Figs. 1(b) and 1(c)]. This asymmetry could be understood using the following arguments.

(1) The measured tunneling spectra result from averaging over the entire Fermi surface. Contrary to tunneling in simple metal, in complex materials such as SCCO, this averaging could be weighted in preferential directions of k space due to particular geometry between the tip and the surface.[16] If this tunneling configuration changes while probing spatially distant points of a sample, this should be followed by a variation in the weighting factors.

(2) In the particular case of SCCO, these variations could generate important modifications of the tunneling spectra. Indeed, when ordered antiferromagnetically, SCCO band structure is found to be a two-band system near the Fermi energy[1,15] [see Fig. 4(b)]. By definition, the gap between both bands will appear to be centered with respect to the Fermi energy if the tunneling current is most sensitive to the nesting points (hot spots). However, this gap will appear to be off centered and larger if the current is most sensitive to the antinodal regions $(\pi,0)$ or $(0,\pi)$ [see full blue arrow, Fig. 4(b)] or the nodal region $(\pi/2,\pi/2)$ direction [see dashed blue arrow, Fig. 4(b)].

We now turn to the temperature dependence of this high energy feature. Figure 3 shows the SCCO spectra of a different optimally doped sample, $x=0.155$ (having a T_c slightly lower than the sample discussed previously in Figs. 1 and 2), at three different temperatures, 5, 27, and 300 K. Considering temperature drifts, the three spectra were taken in the same local region and represent typical results obtained when raising the temperature. At low temperatures, one can

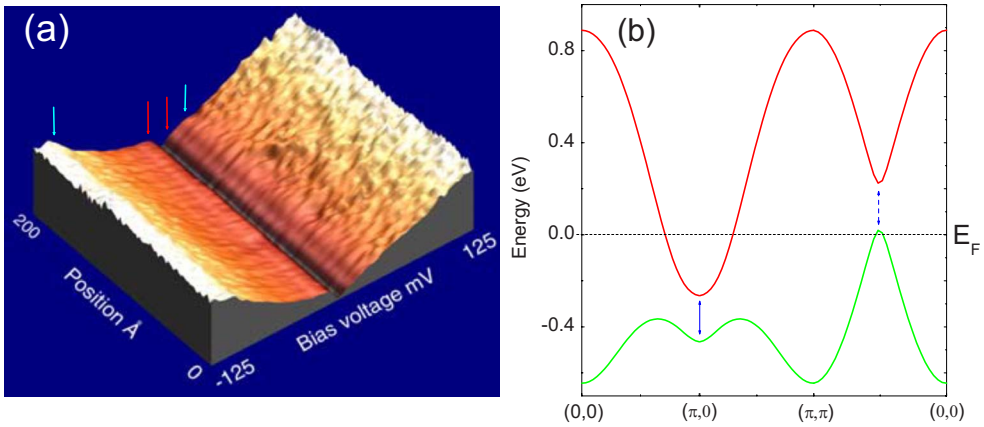

FIG. 4. (Color online) (a) Tunneling spectra following a 200 Å line of SCCO with $x=0.145$ at 5 K [plotted using WSxM (Ref. 17)]. The superconducting gap is identified in the center. The high energy feature can clearly be observed on the negative bias side but only suggested at positive bias [see blue (light gray) arrows]. As explained in (b), this asymmetry relative to zero bias could be explained by the fact that the tunnel current here is mostly sensitive to $(\pi,0)$ or $(0,\pi)$ regions in these measurements. Finally, one can notice that both high and low energy features do not change with position. (b) Band structure calculation of electron-doped cuprate with an AF order using a spin density wave model with a 0.2 eV gap (Refs. 3 and 18). This figure clearly illustrates how the appearance of the AF gap in the tunnel spectra is influenced by the weighted average around the Fermi surface. If the tunnel current is mostly sensitive to the $(\pi,0)$ or $(0,\pi)$ regions, the AF gap is shifted to negative bias (full blue arrow). However, if the tunnel current is mostly sensitive to the diagonal part of the Fermi surface, the AF gap is shifted to positive bias (dashed blue arrow).

again identify two energy scales represented by the red and blue (lower and upper) arrows. When passing above the superconducting transition temperature, the superconducting gap closes but the high energy feature remains. However, when raising the temperature to room temperature, we observe the closing of this energy gap, only leaving the overall U shaped line, similar to the background fit used previously. Since the closing of the large energy pseudogap has been shown to be smooth,[3] it is difficult to identify the characteristic temperature T' above which this feature disappears in the conductance spectra. However, optical measurements of NCCO and PCCO were able to establish the relation $2\Delta'/k_BT'=12$ between the pseudogap energy Δ' and the gap characteristic opening temperature T'. Using this relation and the value $2\Delta'=140$ meV from Fig. 3, one finds $T'=130$K for this sample. This simple estimate of T' explains why one observes the high energy gap at 5 and 27 K but not at 300 K.

Figure 4(a) presents the tunnel spectra taken along a 200 Å line chosen from a topographic and/or spectrographic measurement of a 330 $Å^2$ square. The superconducting gap is observed around zero-bias voltage [see red (dark gray) arrows]. The high energy feature is clearly seen on the negative bias voltage side and is only suggested on the positive bias voltage side [see blue (light gray) arrows].[19] In this scenario, the high energy feature is found to range from −100 to +30 meV, making it comparable in energy (but shifted toward negative bias) with the high energy feature presented in Fig. 1(a) (both spectra were measured in regions close by). Moreover, this image shows that both the high and low energy features are very stable in amplitude throughout nanometer distances. The homogeneity of the superconducting gap magnitude following a 35 nm line scan was previously reported in NCCO.[20] This suggests that the DOS map fluctuation observed in hole-doped cuprates[5,6] is not observed in electron-doped cuprates on the same scale. The variation in the superconducting gap mentioned previously at various distant points on the surface can be explained by slight inhomogeneities in the oxygen content arising in the reduction process.

We have reported the normal state and superconducting state local tunneling spectra of SCCO. On a large scale, the superconducting gap Δ is observed to range from 3.5 to 6 meV, the ratio $2\Delta'/k_BT_c$ thus varying from 4 to 7. At low temperatures, a large energy feature in the tunneling spectra is observed. This one remains above T_c but disappears at higher temperatures. On the nanometer scale, the amplitudes of the superconducting gap and the high energy feature are found not to vary with position. The high energy feature could be the signature of the large energy pseudogap observed by photoemission and optical spectroscopy (interpreted as the signature of AF order). In this case, these results would suggest the coexistence on a local scale of antiferromagnetism and superconductivity. Further measurements need to be performed to confirm this interpretation.

This work was supported by NSF Grants Nos. DMR-0352735 and DMR-0303112 at the University of Maryland. A. Z. acknowledges support from the International Institute for Complex Adaptive Matter (I2CAM), NSF Grant No. DMR-0645461.

*Alexandre.Zimmers@espci.fr

[1] N. P. Armitage *et al.*, Phys. Rev. Lett. **88**, 257001 (2002).
[2] Y. Onose, Y. Taguchi, K. Ishizaka, and Y. Tokura, Phys. Rev. B **69**, 024504 (2004).
[3] A. Zimmers, J. M. Tomczak, R. P. S. M. Lobo, N. Bontemps, C. P. Hill, M. C. Barr, Y. Dagan, R. L. Greene, A. J. Millis, and C. C. Homes, Europhys. Lett. **70**, 225 (2005).
[4] E. M. Motoyama, G. Yu, I. M. Vishik, O. P. Vajk, P. K. Mang, and M. Greven, Nature (London) **445**, 186 (2007).
[5] T. Cren, D. Roditchev, W. Sacks, J. Klein, J.-B. Moussy, C. Deville-Cavellin, and M. Lagues, Phys. Rev. Lett. **84**, 147 (2000); T. Cren, D. Roditchev, W. Sacks, and J. Klein, Europhys. Lett. **54**, 84 (2001); C. Howald, P. Fournier, and A. Kapitulnik, Phys. Rev. B **64**, 100504(R) (2001); S. H. Pan *et al.*, Nature (London) **413**, 282 (2001).
[6] K. McElroy, Jinho Lee, J. A. Slezak, D.-H. Lee, H. Eisaki, S. Uchida, and J. C. Davis, Science **309**, 1048 (2005).
[7] J. S. Higgins, Y. Dagan, M. C. Barr, B. D. Weaver, and R. L. Greene, Phys. Rev. B **73**, 104510 (2006).
[8] L. Alff, Y. Krockenberger, B. Welter, M. Schonecke, R. Gross, D. Manske, and M. Naito, Nature (London) **422**, 698 (2003).
[9] Y. Dagan, M. M. Qazilbash, and R. L. Greene, Phys. Rev. Lett. **94**, 187003 (2005).
[10] G. Blumberg, A. Koitzsch, A. Gozar, B. S. Dennis, C. A. Kendziora, P. Fournier, and R. L. Greene, Phys. Rev. Lett. **88**, 107002 (2002).
[11] H. Matsui, K. Terashima, T. Sato, T. Takahashi, M. Fujita, and K. Yamada, Phys. Rev. Lett. **95**, 017003 (2005).
[12] A. Zimmers, R. P. S. M. Lobo, N. Bontemps, C. C. Homes, M. C. Barr, Y. Dagan, and R. L. Greene, Phys. Rev. B **70**, 132502 (2004); C. C. Homes, R. P. S. M. Lobo, P. Fournier, A. Zimmers, and R. L. Greene, *ibid.* **74**, 214515 (2006).
[13] L. Shan, Y. Huang, Y. L. Wang, Y. Z. Zhang, C. Ren, Shiliang Li, Jun Zhao, Pengcheng Dai, and H. H. Wen, arXiv:cond-mat/0703256 (unpublished).
[14] Y. Dagan, R. Beck, and R. L. Greene, arXiv:cond-mat/0702091 (unpublished).
[15] S. R. Park, Y. S. Roh, Y. K. Yoon, C. S. Leem, J. H. Kim, B. J. Kim, H. Koh, H. Eisaki, N. P. Armitage, and C. Kim, Phys. Rev. B **75**, 060501(R) (2007).
[16] A study of all possible reasons leading to such asymmetries will be pursued in the future.
[17] I. Horcas, R. Fernandez, J. M. Gomez-Rodriguez, J. Colchero, J. Gomez-Herrero, and A. M. Baro, Rev. Sci. Instrum. **78**, 013705 (2007).
[18] Figure courtesy of A. J. Millis.
[19] In some particular line scans, a probable Coulomb blockage is occasionally observed at higher energy but changes with position, making it unrelated to the other spectroscopic features mentioned.
[20] S. Kashiwaya, T. Ito, K. Oka, S. Ueno, H. Takashima, M. Koyanagi, Y. Tanaka, and K. Kajimura, Phys. Rev. B **57**, 8680 (1998).